Evaluation of Bonding Properties Between Cfrp Laminate and Concrete Using Externally Bonded Reinforcement on Transverse Grooves (Ebrotg) Method

Ahmed H. Al-Abdwais * and Adil K. Al-Tamimi

Posted Date: 24 September 2024

doi: 10.20944/preprints202409.1891.v1

Keywords: Bonding strength; (EBROTG) method; Fiber reinforce polymer; Concrete prism; Strengthening.

Article

Evaluation of Bonding Properties between CFRP Laminate and Concrete Using Externally Bonded Reinforcement on Transverse Grooves (EBROTG) Method

Ahmed H. Al-Abdwais [1,2,*] and Adil K. Al-Tamimi [3]

[1] Swinburne University of Technology, Australia
[2] Al-Nahrain University, Baghdad, Iraq;
[3] American University of Sharjah
* Correspondence: Ahmed.h.abdulraheem@nahrainuniv.edu.iq

Abstract: The external bonding system using CFRP composite was widely used for strengthening of different structures worldwide. However, premature debonding in this strengthening technique is the critical failure that leads to the fiber not reaching its ultimate capacity. In order to enhance the capacity of the externally bonded (EB) FRP and to slow the premature debonding failure mechanism, numerous anchoring techniques have been applied to improve the bonding capacity. The externally-bonded reinforcement on grooves (EBROG) technology is one of the strategies that have been recently developed to postponing the debonding issue. Although the extensive studies have been conducted in literature on (EBROG) method, most of these studies have been focused on the bonding characteristics of longitudinal grooves direction, and few studies about effect of different design and configurations (width, height, and spacing) of transverse grooves direction were conducted using only CFRP fabric. In present study, an experimental investigation was carried out to study the bond behavior of the externally bonded reinforcement on transverse grooves (EBROTG) technique on the CFRP-to-concrete joints involving different parameters, including groove width, depth, spaces between grooves, strain values, and bond stress-slip relationships using CFRP laminate. 24 concrete prisms, divided into 8 groups of three specimens, were tested using a single-lap shear test set-up. The result of testing proved that the EBROTG method furnished a proper anchor system and highly enhanced the bonding force of the tests. The increasing range in bond strength with the specimens reinforced by the transverse grooving method was ranging from 11 to 86 % compared with the externally bonded reinforcement (EBR) reflecting the effect of different width, depth and distance between grooves

Keywords: Bonding strength; (EBROTG) method; Fiber reinforce polymer; Concrete prism; Strengthening

1. Introduction

There are various strengthening techniques applied to different structural members worldwide, such as reinforced concrete (RC), timber, steel, and masonry. The most wide speared technique is the externally bonded fiber-reinforced polymer (FRP) composites with structure substrates [1–8]. However, the premature debonding between the fiber and the concrete substrate at the ends is the major phenomena that causing degradation of bonding strength, and consequently reduces the efficiency of utilizing the capacity of FRP material for this strengthening technique.

Therefore, postponing or preventing debonding between concrete substrate and fibre was the major challenge for researcher to provide more efficient utilization for capacity of the fiber reinforcement. For this purpose, anchorage systems are often required to inhibit the delamination of CFRP, prevent peeling-off or separation failure, and increase the capability to transfer the stresses between the CFRP reinforcement and the concrete substrate [9].

 doi:10.20944/preprints202409.1891.v1

Different types of anchoring systems in concrete strengthening field have been utilized over the last decade, including mechanical anchorage, the gradient anchorage system, the fiber-based anchoring method, and near-surface mounted (NSM) anchoring technique [9–17].

Although the efficiency of NSM to prevent the premature debonding due to providing confinement around the FRP, some restrictions including limit of concrete cover that are prevalent in actual circumstances due to existing of stirrups, in addition to the difficulty of prestressing the FRP reinforcement within the grooves that frequently necessitates additional actions.

In 2010, the externally bonded reinforcement on grooves (EBROG) approach was developed, which is targeted to render FRP reinforcing systems more efficient in concrete structures [18]. Such systems were applied in 2010 to ensure the fact that these structures are more efficient compared to the EBR method [18]. In comparison to the traditional externally bonded reinforcement (EBR), the method of externally bonded reinforcement on grooves (EBROG) can reduce the early-age distress that is caused by debonding [18,19]. The contact area between FRP and concrete substrate in EBROG procedure has been increased and bond stresses have been distributed into deeper layers of the substrate. Furthermore, the EBROG method is stated to have a better degree of FRP bonding than traditional EBR techniques [20,21]

Numerous applications have been used to thoroughly examine the EBROG strengthening method, including, beams in flexure [22,23] or shear [24,25], strengthening of reinforced concrete columns subjected to uniaxial loading [26,27] or eccentric loading [28], FRP strengthening of concrete beam-column joints [29], examining the behavior of bond between the FRP sheet and concrete [30,31] and procured FRP sheets [32,33], evaluating the EBROG method's durability [34], moreover, strengthening of heat-damaged concrete [35]. In addition, empirical and analytical models have been developed for EBROG method to estimate the bonding strength between FRP and concrete [36–40]. Furthermore, different factors, including groove width and depth have been investigated to evaluate their effect on the bonding strength [41].

As indicated in literature, most of the studies focused on the bonding properties and the effectiveness of (EBROG) for longitudinal grooves aligned with the direction of the fibre. However, in some cases, execution of long grooves in a straight lines aligned along the specimens is practically difficult process in the field that requires special cutting machine to ensure straight line grooves. Hence, short grooves in transverse direction are good alternative and can be easily applied in practical application. Although the extensive studies on EBROG method recorded in literature, there is lack of significant studies on using transverse grooves method. Few studies have been conducted to assess different depth, width and distance of transverse grooves using only CFRP fabric [42,43]. In this study, the effectiveness of externally bonded CFRP Laminate strips over transverse grooves method has been investigated. The investigation evaluated the bonding strength and failure mode with different parameters including, groove width, depth, distance between grooves, strain variation, and bond slip values. The experimental work includes testing 28 concrete prisms divided into 8 groups of three specimens, one group as a reference and other groups with grooves with different widths, depths of and spaces of, and 80 mm between groove were examined. The results showed significant improvement in bonding strength compared to the results with the use of CFRP fabric.

2. Experimental Program

2.1. Specimens Layout

The experimental program comprised of eight groups of concrete specimens (a total of 24 specimens), each group has three specimens with different parameters. The first group includes the reference of two specimens without grooves. The other groups were grooved in a transverse direction to study various parameters, including different groove depth (4, 8, and 12 mm), width (2, 4, and 6), and the distance between grooves (20, 40, and 80 mm). The concrete prism dimensions are 75 mm x 75 mm x 250 mm. The CFRP laminate were glued externally at one face of the prisms over the transverse grooves with different dimensions and distances between grooves using epoxy adhesive, as reported in Table 1. The thickness of of CFRP laminate was 20 mm wide x 1.4 mm thick and the

 doi:10.20944/preprints202409.1891.v1

bonding lengths was 160 mm. Each bond group was tested using three separate identical specimens labled as "S1" and "S2", and "S3". The specimen's details are illustrated in Table 1. A single-lap shear test set-up was used to perform the test for the specimens.

Table 1. Specimen details.

Groups Designation	No. of Specimens	Groove width mm	Groove depth mm	Distance between grooves mm
G1-R	3	Reference	-	-
G2-(2-4-20)	3	2	4	20
G3-(2-4-40)	3	2	4	40
G4-(4,4,40)	3	4	4	40
G5-(4-4-80)	3	4	4	80
G6-(6-4-40)	3	6	4	40
G7-(4-8-40)	3	4	8	40
G8-(4-12-40)	3	4	12	40
G(w,d,s): Group of Specimens, (width, depth, and spaces between grooves)				

2.2. Materials Properties

In order to manufacture the prisms, the concrete mix design was conducted according to ACI 211.1-91 to achieve the target compressive strength of 40 MPa at 28 days of curing. The test was performed using three cylindrical specimens with 200 heights x 100 mm diameter according to ASTM C39/39M-18 [44]. The CFRP laminate and epoxy adhesive were provided by Sika. The tensile strength of the CFRP strips was determined in accordance to ASTM: D3039 [14]. Tables 2, 3, and 4 show the characteristics of fiber and concrete adhesive, correspondingly.

Table 2. Compressive strength of concrete.

Material	Dimensions (mm)	$f'c$,(MPa)	Tensile strength (MPa)	Modulus of elasticity (MPa)
Concrete		41	3.86	25600

Table 3. Specifications for reinforcing epoxy as stated in the product data sheet [45].

Adhesive	Tensile strength (MPa)	Compressive strength (MPa)	Modulus of elasticity (MPa)
Sikadur-31	30	60	4500

Table 4. Specifications for reinforcing carbon fiber plate as stated in the product data sheet [42].

Material	Dimensions (mm)	Compressive strength, (MPa)	Tensile strength (MPa)	Modulus of elasticity (MPa)
CFRP Laminate	1.4x10 mm	1200	2500	165,000

2.3. Specimens Preparation and Reinforcement

The preparation of the specimens started with drawing the necessary lines for the grooves' places on the concrete surface. The bonding of fiber at the ends of the prism could crack the concrete because of the intense local stresses. In the previous researcher's studies, it is recommended to leaving a distance of 50 mm from the edges of the specimens before applying the glue [46,47] to avoid early cracks in concrete. Two strengthening types were applied: the EBR and. In the EBR the surface was ground using a fine grinder to remove any exposed particles or mortar and cleaned using a high pressure water jet. The layer of adhesive was rubbed on the bonding area, and the fiber was placed. In the method, the grooves were cut using an electric cutting machine equipped with the required

 doi:10.20944/preprints202409.1891.v1

depth, and the grooves were then cleaned from any particles and dust as shown in Figure 1 (a). The bonding was applied by filling the grooves accurately to remove all bubbles inside the adhesive. Finally, the fiber was adhesive and applied to the FRP and the bonding place of the prisms. To enable fixing the gripping steel plates, the CFRP strips were extended by 150 mm from the prism edge. (see Figure 1 (b)). The fiber strips were bonded externally over the grooves, and the curing with 2 weeks was applied for the specimens at room temperature (23ºC). The fiber ends were glued between two steel plates for gripping.

(**a**) (**b**)

Figure 1. Specimens preparation: (a) Cutting grooves; (b) Application of adhesive.

For the purpose of recording the strain values at the CFRP sheets along the bonding length, three strain gauges were installed along the fiber strip in the specimen's direction of load. Figure 2 displays the specimen's dimensions with strain distribution, and Figure 3 shows the instrumented specimen with strain gauges.

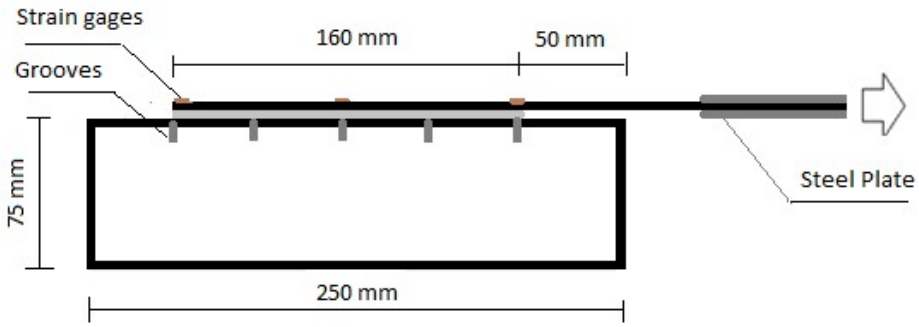

Figure 2. Dimensions and strain gauge plan of the specimens.

 doi:10.20944/preprints202409.1891.v1

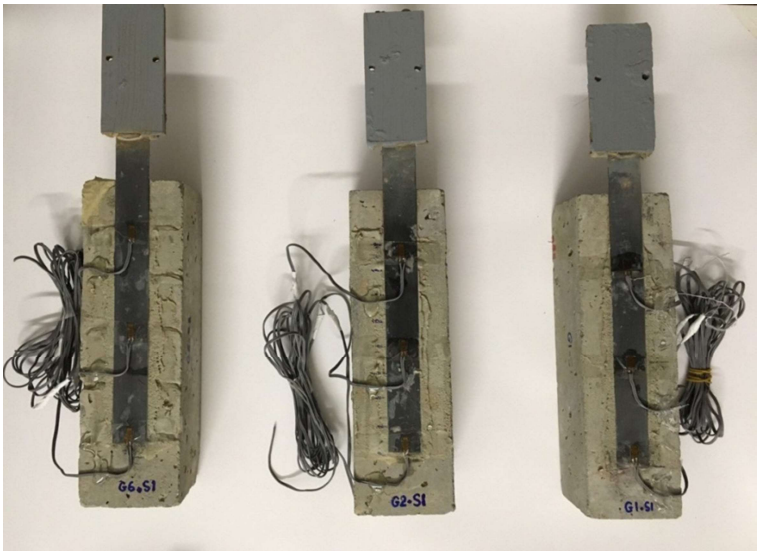

Figure 3. Cured specimens with strain gauges and gripping plates.

2.4. Testing Set-Up

The test of specimens was implemented using a single shear-lap set-up, and the pull-out loading was applied in the structural laboratory using a 100 kN universal testing machine (100 MTS). The application of load was performed on the specimens using displacement control. In order to record the measurement of the load and displacement values, a load cells and extensometers were installed in the testing machine. To guarantee equal elastic elongation of this part, the length of the CFRP laminate outside of the bonding zone were employed to measure the displacement at the loading point.

The alignment of CFRP laminate with the vertical direction of the load was precisely assured in the vertical direction to ensure pure axial loading using laser level to avoid bending moment that may occur on the fiber. The direct tensile test was performed using 2 mm/min of displacement-control loading applied in accordance to the ASTM D3039/D3039M [48]. The set-up dimensions is shown in Figure 4.

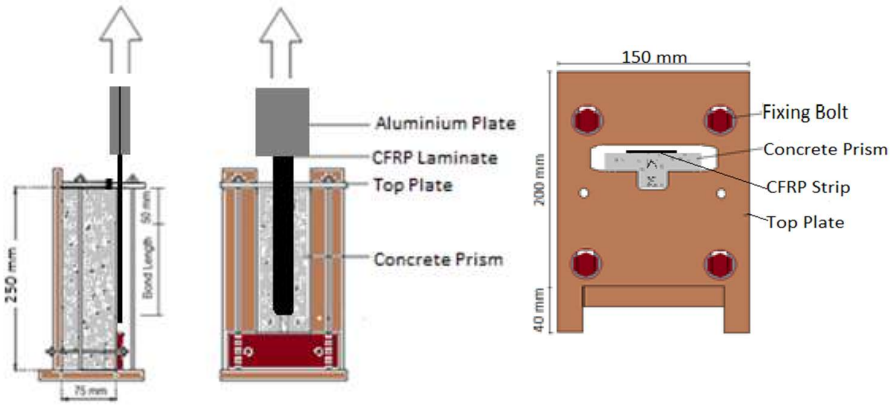

(a) **Side view** (b) **Top view**

Figure 4. Dimensions of Single-lap test set-up.

3. Results and Discussion

3.1. Mode of Failure

 doi:10.20944/preprints202409.1891.v1

In the reference specimen with the EBR method, the failure mode showed detachment of the CFRP from the concrete surface at concrete/adhesive interface (Figure 5), In contrast with grooved specimens of EBROTG method, two types of failure modes have been observed, the debonding of CFRP sheet from concrete surface over the area between the groove occurred at concrete/adhesive interface, and a thin layer has been detached from the concrete surface (similar to the EBR method), while in the area over the grooves, the delamination of the CFRP occurred in the FRP/adhesive interface (Figures 6 –10). This mainly indicate that the weak point of debonding is the interface between concrete and adhesive due detachment of a thin layer from the concrete surface

Figure 5. Failure mode of G1-R.

Figure 6. Failur mode of G2-(2-4-20).

 doi:10.20944/preprints202409.1891.v1

Figure 7. Failure mode of G3-(2-4-40).

Figure 8. Failure mode of G4-(4-4-40).

 doi:10.20944/preprints202409.1891.v1

Figure 9. Failure mode of G5-(2-4-80).

Figure 10. Failure mode of G6-(6-4-40).

In the specimen with a 20 mm distance between grooves (nine grooves), it is clearly observed that the change in the type of debonding along the specimen starting from separation in the fiber/adhesive layer over the grooves to debonding at concrete/adhesive interface at the area between grooves following to the spaces between the grooves (Figure 6).

For the other (EBROTG) specimen with a 40 mm distance between grooves containing five grooves, the change in debonding type along the bonding length followed the spaces between the grooves (Figure 7-10), which indicates the effect of existing grooves to improve the bonding properties by affecting the failure mode at the area over the grooves.

3.2. Bond Strength

 doi:10.20944/preprints202409.1891.v1

Debonding and rupture are two possible ways that FRP can fail, as previously indicated. The sheet's load-bearing capacity, or sheet tensile capacity, is measured at its greatest load when the sheet ruptures, whereas bond strength is the maximum load obtained when the debonding failure occurs. As observed in the test result, the existing of grooves increased the bonding strength due to replacing the failure mode from concrete/adhesive interface to FRP/adhesive interface over the groove section. The ultimate bond strength of all the specimens in this study is presented in Table 5.

Table 5. Specimen designation, specifications, and ultimate bond strength results.

Groups Designation	bg (mm)	dg (mm)	Sg (mm)	Pmax, avg. (kN)	% increase
G1-R	--	--	--	7.53	
G2-(2-4-20)	2	4	20	13.0	72%
G3-(2-4-40)	2	4	40	10.34	37%
G4-(4-4-40)	4	4	40	12.07	60%
G5-(2-4-80)	2	4	80	8.36	11%
G6-(6-4-40)	6	4	40	14.08	86%
G7-(4-8-40)	4	8	40	12.3	63%
G8-(4-12-40)	4	12	40	12.1	60%
G-(bg, dg, Sg): Group of Specimens, (width, depth, and spaces between grooves)					

In the specimens with EBROTG method, the effect of the groove widths 2, 4, and 6 mm of specimens G3-(2-4-40), G4-(4,4,40), and G6-(6-4-40) can be clearly observed in the ultimate strength results of 10.3, 12.07, and 14.08 kN, achieving significant improvement in the bonding properties from 37 to 60% and 86 % respectively compared to the reference specimen. The relationships curves of load versus displacement of the specimens compared to the reference one are presented in Figure 11. This significant increase is reasonable due to increasing the bonding area over the grooves, which indicates a higher tensile strength at the interface between the adhesive and the fiber than that between the fibre and the concrete interface.

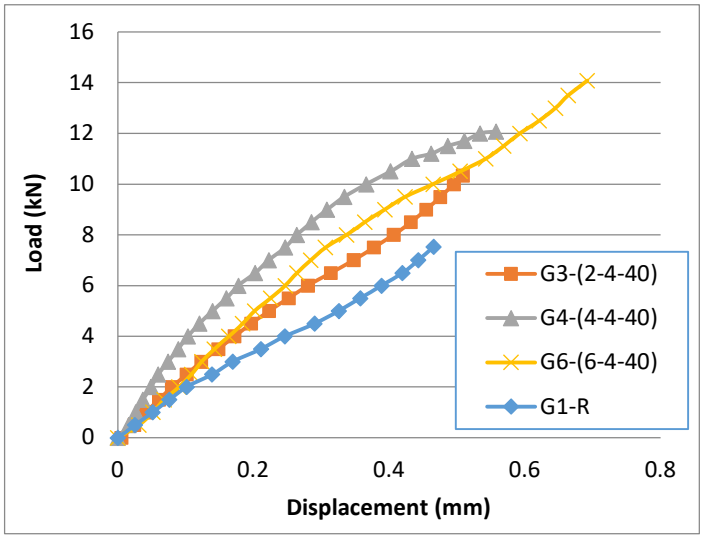

Figure 11. Load-displacement curve of G1, G3, G4, and G5 specimens.

The distance between grooves has significantly affected the bond strength, as indicated in the results of specimens G2 (2-4-20), G3 (2-4-40), and G5 (2-4-80). With increasing the distances from 2, 4, and 8 mm, the bond strength decreased from 13, to 10.34, and 8.36 kN (decrease from 72, to 37, and 11%, respectively, as shown in Figure 12. It has also been shown that the decrease in the bond strength

 doi:10.20944/preprints202409.1891.v1

with increasing the distances between grooves is resulting from reducing the bonding area over the grooves.

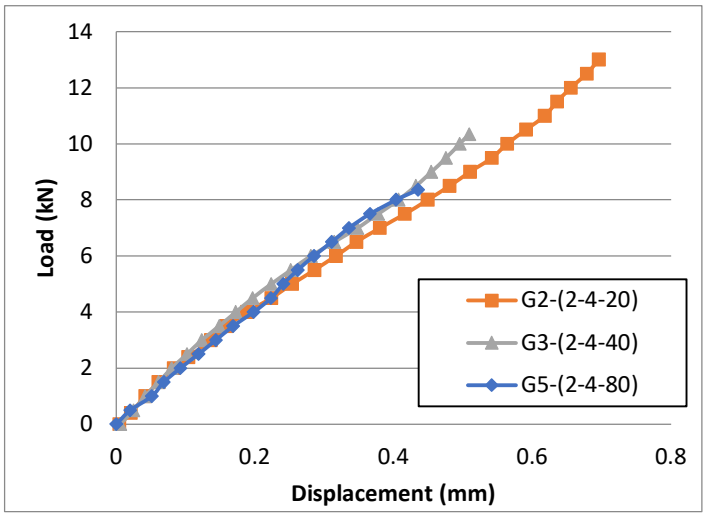

Figure 12. Load-displacement curve of G2, G3, and G5 specimens.

The investigation about the effect of groove depth on the bonding strength was performed for two different depths of 4, 8 and 12 mm in groups G4 (4-4-40), G7 (4-8-40), and G8 (4-12-40) of specimens. The load vs. displacement curve of the results is illustrated in Figure 13. The results were 12.03 and 12.7, and 12.1 kN respectively which indicated no significant influence of the groove depth on the bonding strength results. This can be justified since no failure has occurred surrounding the grooves, as observed in the mode of failure in all specimens.

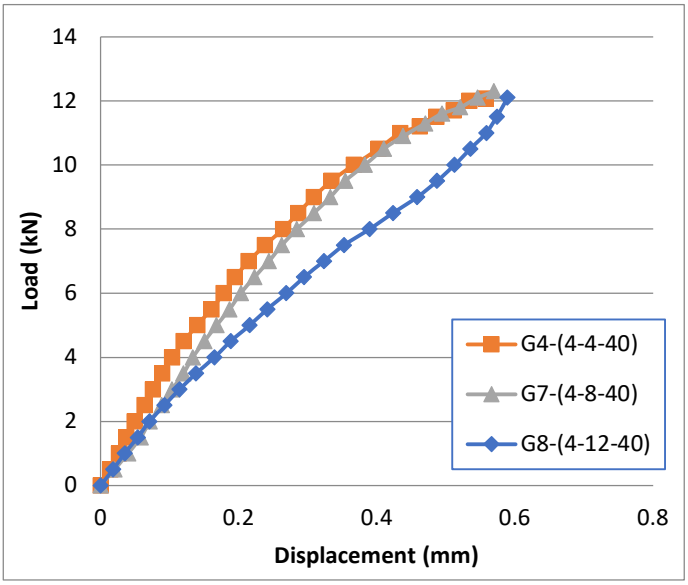

Figure 13. Load-displacement curve of G4, G7, and G8 specimens.

3.3. Strain Values

Through the use of three strain gauges, the strain values were recorded along the 160 mm bond length and along the fiber itself. Strain evolution for EBR and EBROTG specimens is depicted in Figure 14. The highest strain value observed in the EBR specimen had a maximum strain value of 955 microstrain, whereas, the in EBROTG specimens increased between 965 and 1377 microstrain. Since the determination of debonding stress for externally strengthening of FRP, as reported in literature,

 doi:10.20944/preprints202409.1891.v1

is governed by the maximum strain in the fiber, the increase in the strain values for EBROTG specimens prove the effects of existing the grooves for delaying the delamination of fiber from concrete surface depending on the percentage of the grooves area in the bonding surface.

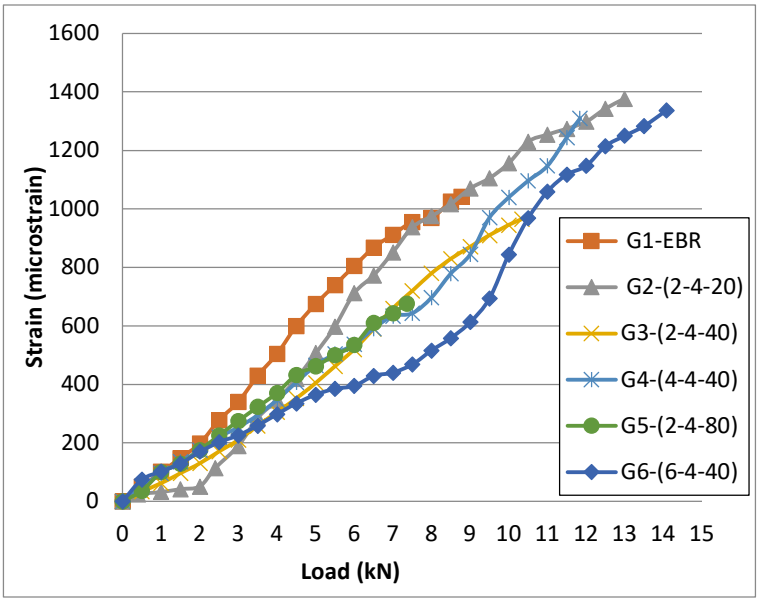

Figure 14. Strain evolution of the (EBR) and (EBROTG) specimens.

3.4. Local Bond Stress-Slip Value

To develop a practical and accurate bond-slip model, it is assumed that the bond stress is uniformly distributed between two constitutive strain gages spaced by Δx_i, and can be calculated using the following formula:

$$\tau_x = E_f . \frac{A_f}{p_f} . \frac{\Delta \varepsilon_i}{\Delta x_i} \quad \text{(Eq. 1)}$$

Where:

E_f is the modulus of elasticity of fiber, A_f is the cross-section area, P_f is the perimeter of the fiber, $\Delta \varepsilon_i$ the difference in strain, and Δx_i is the space between two strain gauges.

The corresponding slip of fiber can be computed using the following formula, by neglecting the strain in the concrete and assuming that the slip at the unloaded end can be ignored before debonding:

$$s = \sum_{k+1}^{n} (\varepsilon_k + \varepsilon_{k+1}) \frac{\Delta x_k}{2} \quad \text{(Eq. 2)}$$

Where:

ε_k and ε_{k+1} are the strain values of two strain gages k, and $k+1$, n represents the total number of strain gages, and Δx_k is the space between two strain gages.

When compared to the experimentally-obtained scattered points and the projected curve using Sena Cruz and Barros's bond-slip equation (Eq. 3) [49,50], the average bond slip and bond stress computed at different positions along the bond length provide a clear and compatible interpretation. The bond-slip values and the predicted curve by the equation for both cases (EBR) and (EBROTG) are depicted in Figure 16 and Figure 17, respectively, illustrating a non-linear ascending pattern up to the maximum value in the bond-slip curves. It can be seen that the bonding in EBROTG method exhibited higher stuffiness compared to EBR method. The experimental and projected values exhibit a strong correlation.

$$\tau(s) = \tau_m \left(\frac{s}{s_m}\right)^a, if\ s \leq s_m \quad \text{(Eq. 3)}$$

where τ_m and s_m are the bond stress and its corresponding slip. a and a' are parameters defining the shape of the curve. The bond-slip curves for the EBR method and method are illustrated in Figures 15 and 16 respectively. In order to provide ideal utilization of bond-slip curve in finite element

 doi:10.20944/preprints202409.1891.v1

modeling, the EBR curve can be used for the bonding area between grooves, representing the failure at the interface between the adhesive and the concrete substrate, while the EBROTG curve will be applied in the bonding area above the groove, representing the failure at the interface between the fiber and the adhesive.

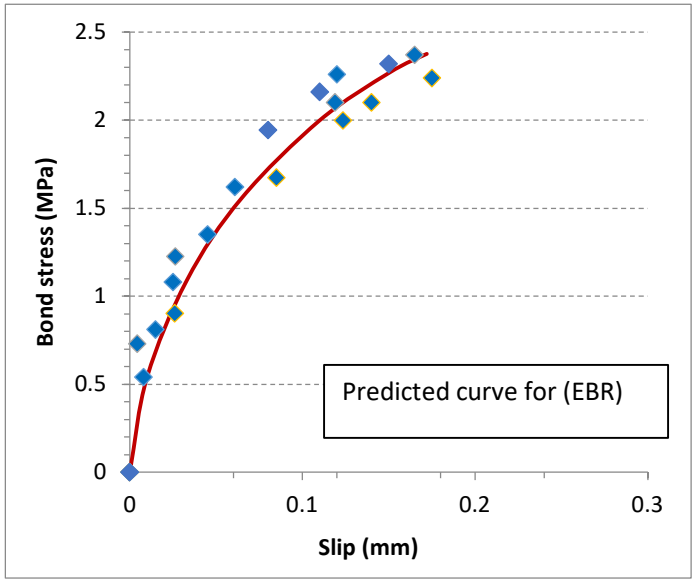

Figure 15. Bond stress-slip relationships for (EBR).

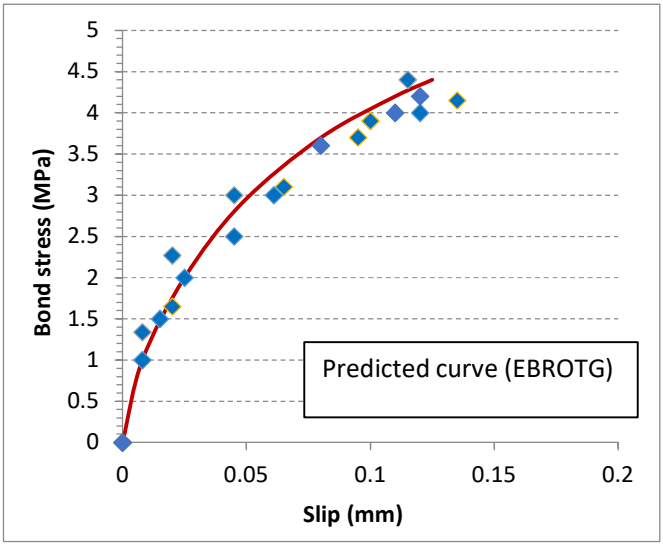

Figure 16. Bond stress-slip relationships for (EBROTG).

4. Conclusions

In this study, 24 concrete specimen was carried out, 3 specimens for EBR and 21 for EBROTG to examine the impact of groove width, depth and distance between grooves on bonding behavior in addition to the strain variation and bond stress-slip relationships. The objective was to find the optimal transverse groove dimensions for EBROTG method in practical application of concrete beam strengthening. The outcomes are as follows:

- The results showed significant improvement in bond strength using EBROTG method by delaying the debonding of the CFRP, when compared specimens strengthened using the EBR

 doi:10.20944/preprints202409.1891.v1

method. The specimens strengthened using the EBROTG approach showed an improvement of 11 to 86% in bond strength according to the groove dimensions.

- The effect of groove width has noteworthy consequence on bond strength. Increasing the groove width between 2, 4, and 6 mm upgraded the bond strength by 37%, 60%, and 86% respectively compared with EBR specimens.
- The distances between grooves with identical groove section dimensions has significant effect by increasing the distances from 2, 4, and 8 mm. The bond strength decreased from 13, to 10.34, and 8.36 kN (from 72%, to 37%, and 11%) respectively. By combining the effects of the width and distances between grooves, it can be concluded that the total cross-section area of the grooves at a certain bonding length and their distribution along this bonding length are the crucial factors in determining the increase in the bonding strength.
- The results indicated no significant increase in bond strength with increasing groove depths since no failure was observed surrounding the grooves.
- The bond stress-slip diagram was extracted from the different strain gages along the bonding length, and the predicted curves can be utilized in finite element modeling of concrete members strengthened with EBROTG method.

Author Contributions: Conceptualization, Ahmed H. Al-Abdwais; Methodology, Ahmed H. Al-Abdwais; Validation, Ahmed H. Al-Abdwais and Adil K. Al-Tamimi; Formal analysis, Ahmed H. Al-Abdwais; Resources, Ahmed H. Al-Abdwais; Writing – original draft, Ahmed H. Al-Abdwais; Writing – review & editing, Adil K. Al-Tamimi; Funding acquisition, Adil K. Al-Tamimi. All authors have read and agreed to the published version of the manuscript.

Data Availability Statement: The original contributions presented in the study are included in the article, further inquiries can be directed to the corresponding authors.

Acknowledgments: I would like to express my great appreciation and acknowledgement to civil engineering department in the American University of Sharjah for their technical support during the research period.

Declaration of Competing Interest: The author declare that they have no known competing financial interests or personal relationships that could have appeared to influence the work reported in this paper.

References

1. Meier U. Strengthening of structures using carbon fibre/epoxy composites. Construction and Building Materials. 1995;9(6), pp.341-51.
2. Yao J, Teng J. Plate end debonding in FRP-plated RC beams—I: Experiments. Engineering Structures. 2007;29(10), pp.2457-71.
3. Tajmir-Riahi A, Moshiri N, Mostofinejad D. Inquiry into bond behavior of CFRP sheets to concrete exposed to elevated temperatures–Experimental & analytical evaluation. Composites Part B: Engineering. 2019.
4. Gao P, Gu X, Mosallam AS. Flexural behavior of preloaded reinforced concrete beams strengthened by prestressed CFRP laminates. Composite Structures. 2016;157: pp.33-50.
5. Martinelli E, Hosseini A, Ghafoori E, Motavalli M. Behavior of prestressed CFRP plates bonded to steel substrate: Numerical modeling and experimental validation. Composite Structures. 2019;207: pp.974-84.
6. Hosseini A, Nussbaumer A, Motavalli M, Zhao X-L, Ghafoori E. Mixed mode I/II fatigue crack arrest in steel members using prestressed CFRP reinforcement. International Journal of Fatigue. 2019.
7. Mosallam A, Banerjee S. Enhancement in in-plane shear capacity of unreinforced masonry (URM) walls strengthened with fiber reinforced polymer composites. Composites Part B: Engineering. 2011;42(6): pp.1657-70.
8. Hosseini A, Mostofinejad D, Emami M. Influence of bonding technique on bond behavior of CFRP-to-clay brick masonry joints: Experimental study using particle image velocimetry (PIV). International Journal of Adhesion and Adhesives. 2015; pp.59:27-39.
9. Ali A, Abdalla J, Hawileh R, Galal K. CFRP mechanical anchorage for externally strengthened RC beams under flexure. Physics Procedia. 2014; pp.55:10-6.
10. Yu P, Silva PF, Nanni A. Description of a mechanical device for prestressing of carbon fiber-reinforced polymer sheets-Part I. ACI Structural Journal. 2008;105(1):3-10.
11. Michels J, Martinelli E, Czaderski C, Motavalli M. Prestressed CFRP strips with gradient anchorage for structural concrete retrofitting: experiments and numerical modeling. Polymers. 2014;6(1): pp.114-31.
12. Pham HB, Al-Mahaidi R. Prediction models for debonding failure loads of carbon fiber reinforced polymer retrofitted reinforced concrete beams. Journal of composites for construction. 2006;10(1): pp.48-59.

13. Kim YJ, Wight RG, Green MF. Flexural strengthening of RC beams with prestressed CFRP sheets: Development of nonmetallic anchor systems. Journal of Composites for Construction. 2008;12(1): pp.35-43.
14. Michels J, Sena-Cruz J, Czaderski C, Motavalli M. Structural strengthening with prestressed CFRP strips with gradient anchorage. Journal of Composites for Construction.2013;17(5): pp.651-61.
15. Bilotta A, Ceroni F, Di Ludovico M, Nigro E, Pecce M, Manfredi G. Bond efficiency of EBR and NSM FRP systems for strengthening concrete members. Journal of Composites for Construction. 2011;15(5): pp.757-72.
16. Hajihashemi A, Mostofinejad D, Azhari M. Investigation of RC beams strengthened with prestressed NSM CFRP laminates. Journal of Composites for Construction.2011;15(6): pp.887-95.
17. Al-Abdwais A. and Al-Mahaidi, R. Experimental and finite element analysis of flexural performance of RC beams retrofitted using near-surface mounted with CFRP composites and cement adhesive, Engineering Structures, 241(1) (2021): 112429.
18. Mostofinejad D, Mahmoudabadi E. Grooving as alternative method of surface preparation to postpone debonding of FRP laminates in concrete beams. Journal of Composites for Construction. 2010;14(6): pp.804-11.
19. Mostofinejad D, Shameli SM, Hosseini A. EBROG and EBRIG methods for strengthening of RC beams by FRP sheets. European Journal of Environmental and Civil Engineering. 2014;18(6): pp.652-68.
20. Moshiri N, Tajmir-Riahi A, Mostofinejad D, Czaderski C, Motavalli M. Experimental and analytical study on CFRP strips-to-concrete bonded joints using EBROG method. Composites Part B: Engineering. 2019;158: pp.437-47.
21. Tajmir-Riahi A, Moshiri N, Mostofinejad D. Bond mechanism of EBROG method using a single groove to attach CFRP sheets on concrete. Construction and Building Materials. 2019;197: pp.693-704.
22. Mostofinejad D, Shameli SM. Externally bonded reinforcement in grooves (EBRIG) technique to postpone debonding of FRP sheets in strengthened concrete beams. Construction and Building Materials. 2013;38: pp.751-8.
23. Czaderski C, Moshiri N, Hosseini A, Mostofinejad D, Motavalli M. EBROG technique to enhance the bond performance of CFRP strips to concrete substrate. SMAR 2019-Fifth conference on Smart Monitoring, assessment and rehabilitation of civil structures, 712 Potsdam Berlin, Germany. Potsdam, Berlin, Germany2019.
24. Shomali A, Mostofinejad D, Esfahani MR. Experimental and numerical investigation of shear performance of RC beams strengthened with FRP using grooving method. Journal of Building Engineering. 2020:101409.
25. Mostofinejad D, Hosseini SA, Razavi SB. Influence of different bonding and wrapping techniques on performance of beams strengthened in shear using CFRP reinforcement. Construction and Building Materials. 2016;116: pp.310-20.
26. Moshiri N, Hosseini A, Mostofinejad D. Strengthening of RC columns by longitudinal CFRP sheets: Effect of strengthening technique. Construction and Building Materials. 2015;79: pp.318-25.
27. Mostofinejad D, Moshiri N. Compressive strength of CFRP composites used for strengthening of RC columns: Comparative evaluation of EBR and grooving methods. Journal of Composites for Construction. 2014;19(5):04014079.
28. NoroozOlyaee M, Mostofinejad D. Slenderness Effects in Circular RC Columns Strengthened with CFRP Sheets Using Different External Bonding Techniques. Journal of Composites for Construction. 2019;23(1):04018068.
29. Ilia E, Mostofinejad D. Seismic retrofit of reinforced concrete strong beam–weak column joints using EBROG method combined with CFRP anchorage system. Engineering Structures. 2019;194: pp.300-19.
30. Tajmir-Riahi A, Mostofinejad D, Moshiri N. Bond resistance of a single groove in EBROG method to attach CFRP sheets on concrete. Proceedings of the ninth international conference on fibre-reinforced polymer (FRP) composites in civil engineering (CICE 2018), Paris, France, 2018, Pp.368-73.
31. Hosseini A, Mostofinejad D. Experimental investigation into bond behavior of CFRP sheets attached to concrete using EBR and EBROG techniques. Composites Part B: Engineering. 2013;51:130-9.
32. Moshiri N, Mostofinejad D, Tajmir-Riahi A. Bond behavior of pre-cured CFRP strips to concrete using externally bonded reinforcement on groove (EBROG) method. Proceedings of the ninth international conference on fibre-reinforced polymer (FRP) composites in civil engineering (CICE 2018), Paris, France, 2018, pp. 361-7.
33. Moshiri N, Czaderski C, Mostofinejad D, Motavalli M. Bond strength of prestressed CFRP strips to concrete substrate: comparative evaluation of EBR and EBROG methods. SMAR 2019-Fifth Conference on Smart Monitoring, Assessment and Rehabilitation of Civil Structures. Potsdam, Berlin, Germany, 2019.
34. Mostofinejad D, Mohammadi M. Effect of Freeze–Thaw Cycles on FRP-Concrete Bond Strength in EBR and EBROG Systems. Journal of Composites for Construction. 2020;24(3):04020009.
35. Tajmir-Riahi A, Moshiri N, Mostofinejad D. EBROG method to strengthen heat751damaged concrete with CFRP sheets. SMAR 2019-Fifth Conference on Smart Monitoring, Assessment and Rehabilitation of Civil Structures. Potsdam, Berlin, Germany2019.

 doi:10.20944/preprints202409.1891.v1

36. Moghaddas A, Mostofinejad D. Empirical FRP-Concrete Bond Strength Model for Externally Bonded Reinforcement on Grooves. Journal of Composites for Construction. 2018;23(2):04018080.
37. Amirezza M., Davood M., Alireza S. An empirical FRP-concrete bond-slip model for externally-bonded reinforcement on grooves. Construction and Building Materials Journal. 2021;281; pp.1-19.
38. Heydari Mofrad M, Mostofinejad D, Hosseini A. A generic non-linear bond-slip model for CFRP composites bonded to concrete substrate using EBR and EBROG techniques. Composite Structures. 2019;220: pp.31-44.
39. Tajmir-Riahi A, Moshiri N, Czaderski C, Mostofinejad D. Effect of the EBROG method on strip-to-concrete bond behavior. Construction and Building Materials. 2019;220:701-11.
40. Niloufar M, et al. Bond Behavior of Prestressed CFRP Strips-to-Concrete Joints Using the EBROG Method: Experimental and Analytical Evaluation, Journal of Composites for Construction, Volume 27(1), 2022, pp.1-17.
41. Shakiba Z, Davood M., Nicolas F. Experimental evaluation of FRP-concrete bond using externally-bonded reinforcement on grooves (EBROG) method. Composite Structure Journal. 2023; 310; pp.1-17.
42. Fatemeh M. and Davood M. Groove classification in EBROG FRP-to-concrete joints. Construction and Building Materials. 2021, Volume 275, pp.1-15.
43. Fatemeh M. et al. Effect of Different Groove Classes Used in Externally Bonded Reinforcement on Grooves Joints on Carbon Fiber-Reinforced Polymer-to-Concrete Bond Behavior, 2022, Volume 119(4), pp.123-140.
44. ASTM C39/C39M-18. Standard Test Method for Compressive Strength of Cylindrical Concrete Specimens. ASTM International, West Conshohocken, PA.
45. Sika group. www.sika.com
46. Ali-Ahmad M, Subramaniam K, Ghosn M. Experimental investigation and fracture analysis of debonding between concrete and FRP sheets. J Eng Mech 2006;132(9): pp.914–23.
47. Mazzotti C, Savoia M, Ferracuti B. An experimental study on delamination of FRP plates bonded to concrete. Constr Build Mater 2008;22(7):1409–21.
48. ASTM D3039/D3039M-17. Standard Test Method for Tensile Properties of Polymer Matrix Composite Materials. ASTM International, 2017.
49. Sena Cruz J. and J. Barros. “Modeling of bond between near-surface mounted CFRP laminate strips and concrete.” Computers and Structures. 2004; 82, pp.1513-1521.
50. Sena Cruz J. and J. Barros. “Bond Between Near-Surface Mounted Carbon-Fiber-Reinforced Polymer Laminate Strips and Concrete.” Journal of Composites for Construction. 2004, 8(6), pp. 519-527.